# Al6061-RAM2 Development and Hot-Fire Testing using Additive Manufacturing Laser Powder Directed Energy Deposition for Liquid Rocket Engine Channel-Cooled Nozzles

Tessa M. Fedotowsky<sup>1</sup>, Ben B. Williams<sup>2</sup>, Paul R. Gradl<sup>3</sup>, Darren C. Tinker<sup>4</sup> NASA Marshall Space Flight Center, Huntsville, AL 35812

> Jeremy Iten,<sup>5</sup> Anthony Manerbino,<sup>6</sup> Adam Polizzi<sup>7</sup> Elementum 3D, Erie CO 80516

Aluminum 6061-RAM2 is a high-strength aluminum feedstock developed for additive manufacturing (AM) processes. This alloy leverages Reactive Additive Manufacturing (RAM) technology. The RAM aluminum alloys were developed to be weldable—therefore printable—while equaling or exceeding strength properties of high strength wrought aluminum alloys. NASA and industry partners developed Laser Powder Directed Energy Deposition (LP-DED) additive manufacturing of Al6061-RAM2 for use in aerospace applications. Efforts included establishing build parameters, characterizing the alloy, fabricating components, and completing hot-fire testing of complex internal channel-cooled nozzles. These efforts are to address the growing need for large-scale parts using high-performance light-weight materials. Two rocket engine nozzles were fabricated using LP-DED Al6061-RAM2 that included integral cooling channels. The Al6061-RAM2 has completed process development and initial properties were established. This paper provides an overview of the LP-DED process development, material characterization and properties, component manufacturing, supplemental development, and hot-fire testing. Results from hot-fire testing are provided for a lander-class 31 kN (7,000 lbf) thrust engine using Liquid Oxygen (LOX)/Liquid Hydrogen (LH2) and LOX/Methane (LCH4).

#### **Nomenclature**

ACO = Announcement of Collaborative Opportunity

AM = Additive Manufacturing or Additively Manufactured

CASI = Compact Augmented Spark Impinging

CMP = Chemical Mechanical Polishing

CT = Computed Tomography

CTE = Coefficient of Thermal Expansion

EB = Electron Beam

GCD = Game Changing Development GTAW = Gas Tungsten Arc Welding

HEE = Hydrogen Embrittlement Environment

HIP = Hot Isostatic Pressing
ICP = Inductivity Coupled Plasma
L-PBF = Laser Powder Bed Fusion

LP-DED = Laser Powder Directed Energy Deposition

LOX = Liquid Oxygen

1

<sup>&</sup>lt;sup>1</sup> AST, Structural Dynamics, Mail Stop ER41, NASA Marshall Space Flight Center. Member.

<sup>&</sup>lt;sup>2</sup> AST, Liquid Propulsion Engineer, Mail Stop ER13, NASA Marshall Space Flight Center. Member.

<sup>&</sup>lt;sup>3</sup> Principal Engineer, Engine Systems Component Technology Branch, Associate Fellow, AIAA

<sup>&</sup>lt;sup>4</sup> AST, Liquid Propulsion Engineer, Mail Stop ER13, NASA Marshall Space Flight Center. Member.

<sup>&</sup>lt;sup>5</sup> Chief Technical Officer, Elementum 3D.

<sup>&</sup>lt;sup>6</sup> Senior Materials and Application Engineer, Elementum 3D.

<sup>&</sup>lt;sup>7</sup> Engineering Manager, Elementum 3D.

#### AIAA SciTech, 8-12 January 2024, Orlando, FL

MPEA = Multi-Principal Element Alloy

MR = Mixture Ratio

MSFC = Marshall Space Flight Center

MTD = Manufacturing Technology Demonstrators

NHT = No Heat Treatment

ODS = Oxide Dispersion Strengthening

Pc = Chamber Pressure

RAMFIRE = Reactive Additive Manufacturing for Fourth Industrial Revolution Exploration Systems

STMD = Space Technology Mission Directorate

TCA = Thrust Chamber Assembly
TIG = Tungsten Insert Gas

TRL = Technology Readiness Level UTS = Ultimate Tensile Strength

YS = Yield Strength

#### I. Introduction

The NASA Marshall Space Flight Center (MSFC) has applied various forms of metallic additive manufacturing (AM) for liquid rocket engine component design, development, and testing since ~2010 [1]. These AM processes were demonstrated to significantly reduce hardware cost, shorten fabrication schedules, increase reliability by reducing the number of joints, and improve hardware performance by allowing unconventional design complexity. The use of Laser Powder Directed Energy Deposition (LP-DED) expands the possibilities for designing and building large-scale components, particularly regeneratively cooled liquid rocket nozzles that incorporate integral cooling channels [2].

The Reactive Additive Manufacturing for Fourth Industrial Revolution Exploration Systems (RAMFIRE) project matured material and manufacturing technologies for large-scale lightweight AM aluminum, providing significant weight savings for engines and launch vehicles. RAMFIRE was a joint effort with Elementum 3D under a Space Technology Mission Directorate (STMD) Announcement for Collaborative Opportunity (ACO) with industry through public-private partnerships to design and manufacture channel-cooled nozzles. The project specifically matured LP-DED AM for Al6061-RAM2, which is now commercially available, and three commercial DED vendors have successfully developed printing parameters.

The RAMFIRE project focused on five key areas:

- LP-DED Al6061-RAM2 feedstock specification and verification
- LP-DED process development and validation
- Printed Al6061-RAM2 microstructural and mechanical property characterization
- Hot-fire testing of a 31 kN (7,000-lb<sub>f</sub>) thrust class regeneratively cooled nozzle
- Printing of a large-scale regeneratively cooled demonstrator nozzle

The lander-scale RAMFIRE thrust chamber assembly (TCA) included an igniter, injector, chamber, and nozzle and is shown in Figure 1. A compact augmented spark impinging (CASI) igniter was used for ignition. A GRX-810 (Ni-Co-Cr) pentad impinging injector was printed using Laser Powder Bed Fusion (L-PBF). GRX-810 is a NASA-developed multi-principal element alloy (MPEA), that uses oxide dispersion strengthening (ODS) [3]. A GRCop-42 L-PBF printed chamber was used based on a heritage design from prior NASA test projects [4,5]. The focus of hot-fire testing was a LP-DED Al6061-RAM2 nozzle. The Al6061-RAM2 channel-cooled nozzle design overview is shown in Figure 2. The nozzle assembly was designed with a base LP-DED Al6061-RAM2 nozzle liner with integral channels, two traditionally manufactured Al6061-T6 manifolds, and eight explosively bonded Inconel 625 to Al6061-T6 ports. The 31 kN (7,000 lb<sub>f</sub>) thrust class hardware was hot-fire tested with liquid oxygen (LOX)/liquid hydrogen (LH2) and LOX/liquid methane (LCH4). The thrust chamber assembly accumulated a total duration of 577 seconds through 22 hot-fire tests with the longest single duration of 60 seconds.

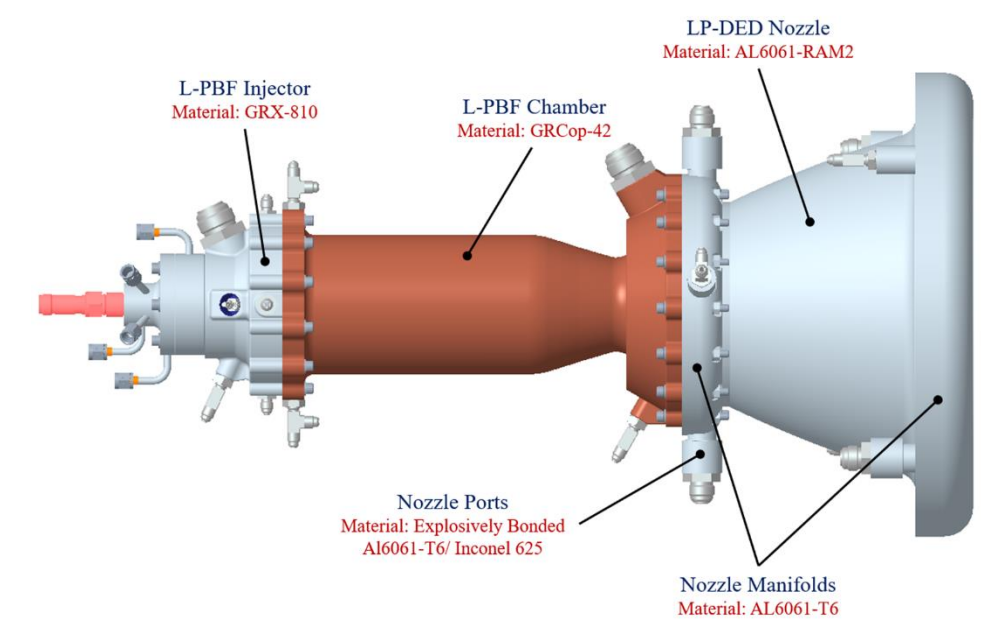


Figure 1. RAMFIRE thrust chamber assembly.

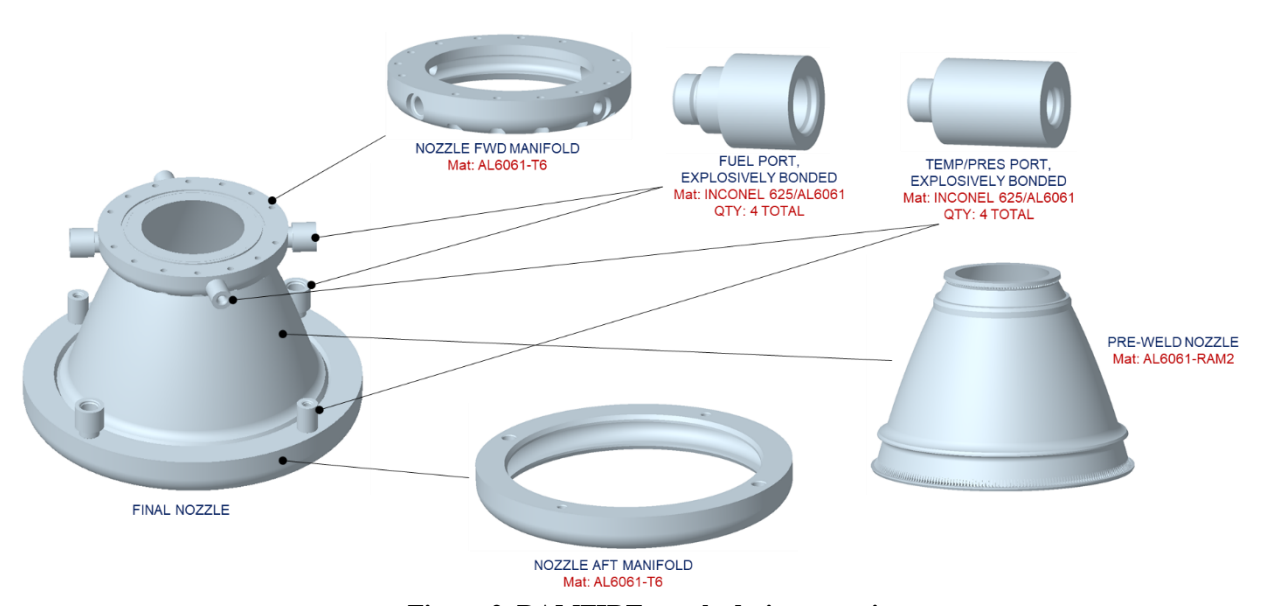


Figure 2. RAMFIRE nozzle design overview.

# II. AL6061-RAM2 Background and LP-DED Development

Aluminum has several attractive characteristics for aerospace AM applications such as high thermal conductivity, good corrosion resistance, mechanical properties offering high strength/weight, and hydrogen embrittlement environment (HEE) resistance. Unfortunately, most traditional wrought high-strength alloys, such as aluminum, suffer from hot tearing (solidification cracking) if additively manufactured or otherwise melted. In short, unaltered aluminum alloys have considerable drawbacks for AM applications. Al6061-RAM2 is an aluminum alloy that provides excellent ductility, high strength at low and high temperatures, and good thermal conductivity when used with AM processes [6]. The alloy is made by a Reactive Additive Manufacturing (RAM) process that blends gasatomized 6061 base powder with ceramic particulates [7]. For Al6061-RAM2, 6061 particles are blended with 2%

volume of Boron Carbide (B4C) and Titanium (Ti)-rich particulates. The RAM process inoculates alloys against hot tearing and produces an equiaxed fine-grained microstructure.

Previously, this Al6061-RAM2 feedstock was developed for use in L-PBF, but MSFC and industry partners under the RAMFIRE project matured the alloy for LP-DED use, including powder feedstock and material characterization. The chemical composition of Al6061-RAM2 additive powder used in this project is shown in Table 1. The chemical composition was obtained using inductivity coupled plasma (ICP).

Initial LP-DED trials were not successful due to powder flowability issues. The powder was not spherical, and the Hall flow values were approximately twice of the acceptable range for LP-DED. Hall Flow, Particle Size Analysis, and powder morphology via optical microscopy was performed to understand the differences. Powder morphology analysis was completed including particle size distribution, sphericity, and other shape properties that can affect the powder's flowability during AM processing. The selected acceptable powder size distribution and associated Hall Flow times are shown in Table 2.

Table 1. Chemical composition of Al6061-RAM2 (LP-DED) vs. (L-PBF).

|               | Al6061-RAM2 | Al6061-RAM2 |  |  |
|---------------|-------------|-------------|--|--|
|               | (LP-DED)*   | (L-PBF)*    |  |  |
| Element       | Wt. %       |             |  |  |
| Al            | 94.61       | 94.67       |  |  |
| В             | 0.74        | 0.74        |  |  |
| C             | 0.18        | 0.18        |  |  |
| Cr            | 0.07        | 0.10        |  |  |
| Cu            | 0.26        | 0.28        |  |  |
| Fe            | 0.17        | 0.09        |  |  |
| Mg            | 0.83        | 0.84        |  |  |
| Mn            | 0.01        | 0.00        |  |  |
| Si            | 0.56        | 0.54        |  |  |
| Ti            | 2.45        | 2.44        |  |  |
| Zn            | 0.00        | 0.01        |  |  |
| Others, Each  | < 0.05      | < 0.05      |  |  |
| Others, Total | < 0.16      | < 0.16      |  |  |

\*From a one powder lot; not specification values

Table 2. Powder feedstocks for Al6061 and Al6061-RAM2 (LP-DED).

|                      | Powd     | Average Hall |          |               |
|----------------------|----------|--------------|----------|---------------|
| Material             | D10 [µm] | D50 [µm]     | D90 [μm] | Flow Time [s] |
| Base 6061 (LP-DED)   | 46.4     | 67.6         | 96.0     | 59.6          |
| Al6061-RAM2 (LP-DED) | 44.3     | 67.3         | 96.3     | 59.7          |

Material characterization was completed including microstructure, evaluation of heat treatment steps, and mechanical testing. Microstructure and mechanical properties were obtained from thin-wall ( $\sim$ 1.5 mm / 0.060"), single bead build boxes. Microstructure samples were obtained after each heat treatment step to characterize the as-built, post-hot isostatic pressing (HIP), post-Solution, and fully heat-treated (age hardened) condition. Equiaxed, fine grains were observed in all the conditions and the mean grain size for LP-DED Al6061-RAM2 is  $\sim$ 5  $\mu$ m shown in Figure 3. The addition of B4C and Ti inoculant particles provides heterogenous nucleation sites for solidification, which causes refinement of the grain structure and formation of equiaxed grains. Mean grain sizes were larger for LP-DED samples, 5  $\mu$ m, compared to L-PBF samples, 1.5  $\mu$ m, shown in Figure 4. The grain size from both printing processes did not significantly change after heat treatment because the inoculant particles acted as grain boundary pinners.

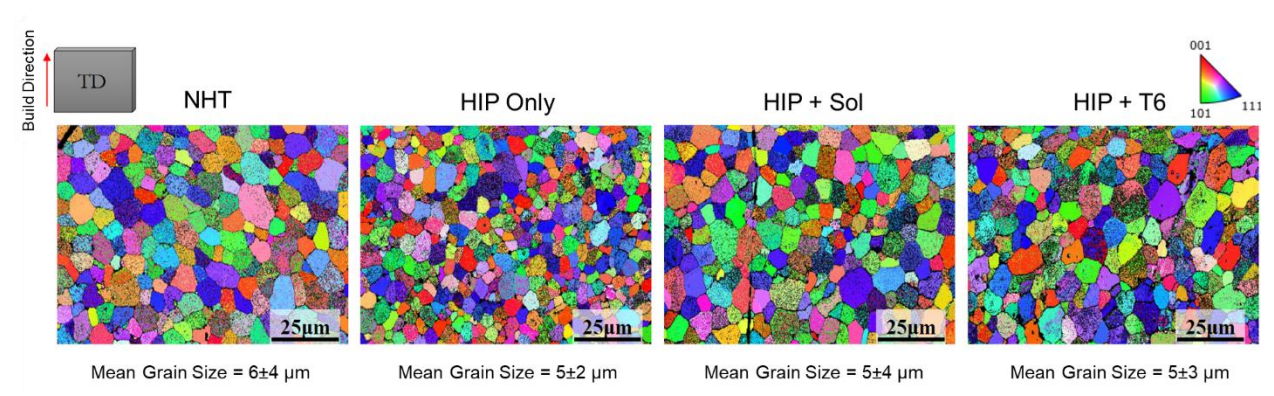


Figure 3. Microstructure results for LP-DED Al6061-RAM2.

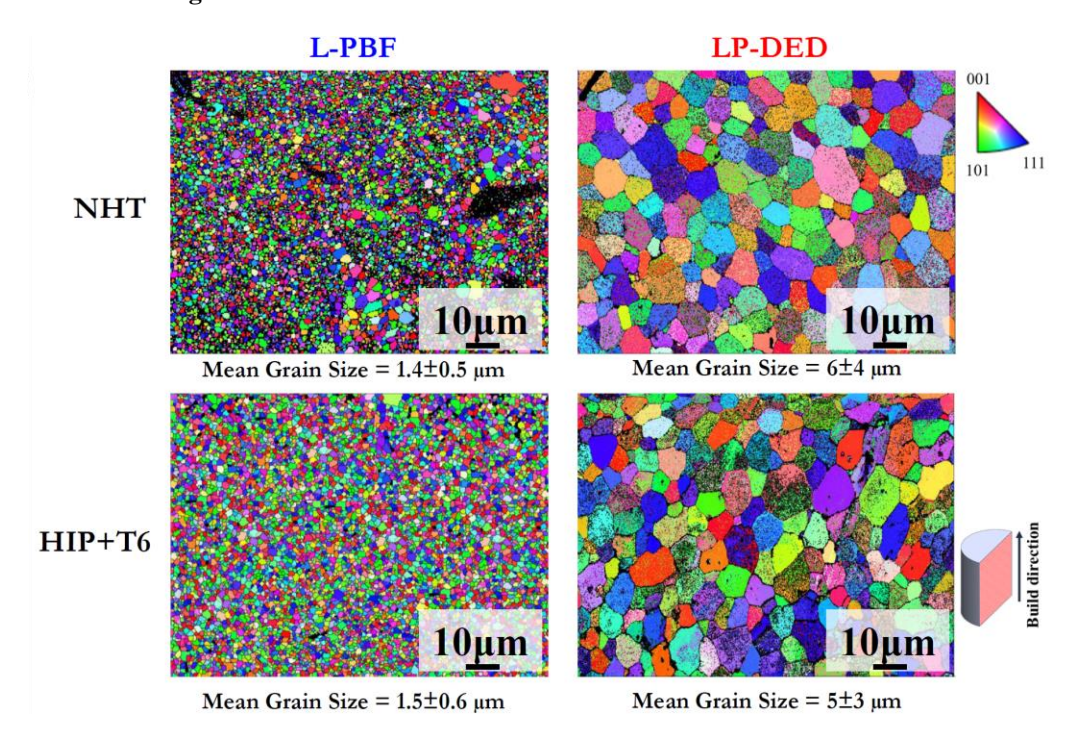


Figure 4. Microstructure of LP-DED samples compared to L-PBF samples.

Tensile property data is shown in Figure 5 and were in the fully heat-treated condition (HIP + T6). The surfaces of the test specimens were machined to mitigate surface texture variation from the as-built condition. Two different conditions, non-anodized and anodized, were examined parallel to the build direction (vertical) and perpendicular (horizontal). The anodized condition was only examined parallel to the build direction. Ultimate tensile strength (UTS) and 0.2% yield strength (YS) are higher for the horizontal non-anodized samples at -196°C (-320°F), then are comparable after 24°C (75°F). UTS and YS decreased with the increase of test temperatures, as expected. The anodization condition seems to have little effect on mechanical properties of the LP-DED Al6061-RAM2. The vertical and horizontal non-anodized conditions show minor differences in material properties, specifically for ultimate strength, yield strength, and percent elongation.

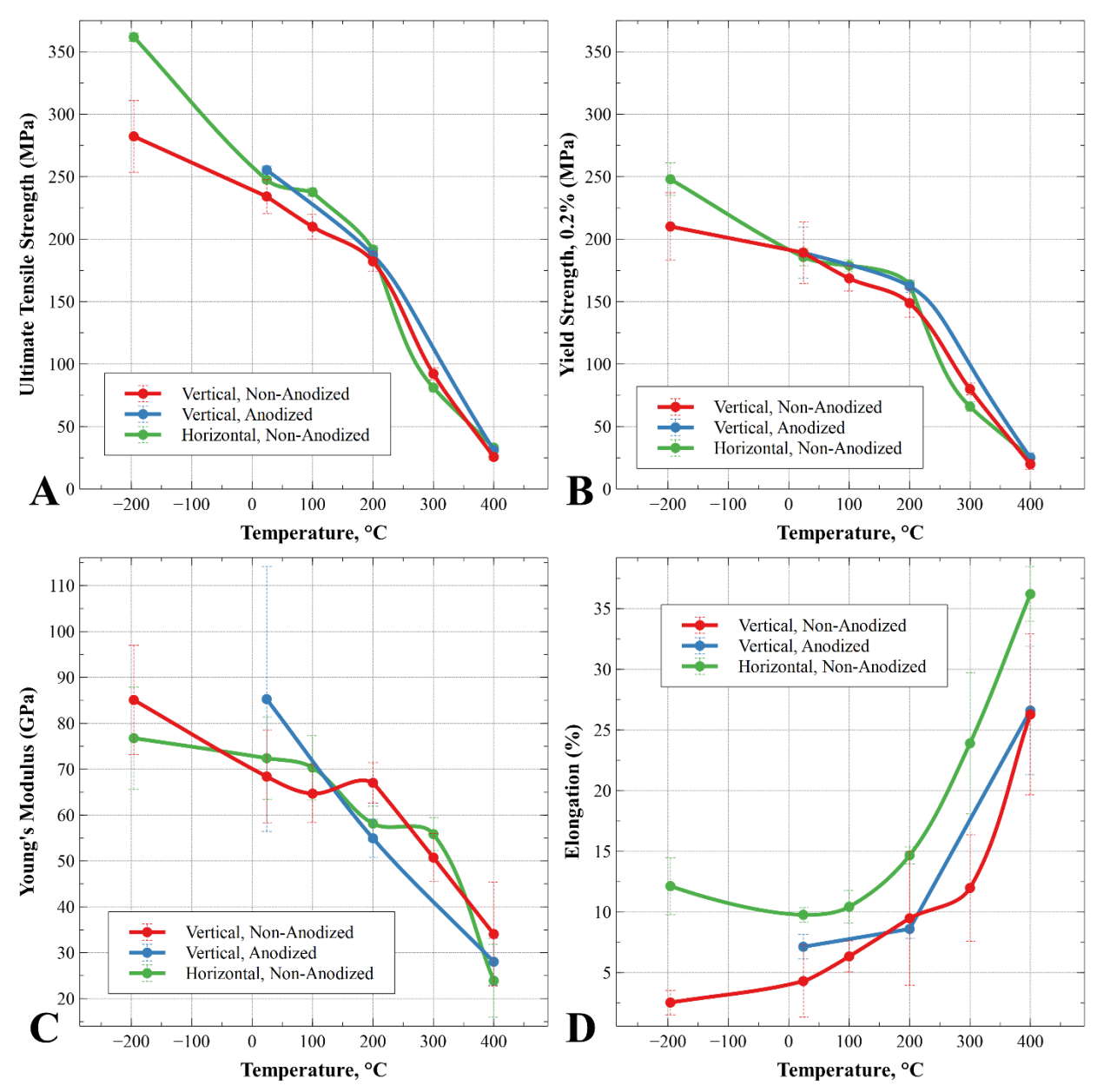


Figure 5. Mechanical testing results of LP-DED Al6061-RAM2. A: Ultimate Tensile Strength; B: Yield Strength; C: Young's Modulus; D: Elongation (%).

The coefficient of thermal expansion (CTE) properties of Al6061-RAM2 and wrought Al6061-T6 are shown in Table 3. All properties were tested in T6 heat treated condition.

Table 3. Coefficient of Thermal Expansion properties.

|                      | CTE [µm/m/°C] |       |  |
|----------------------|---------------|-------|--|
| Material             | 50°C          | 100°C |  |
| Al6061-RAM2 (LP-DED) | 21.8          | 22.2  |  |
| Al6061-RAM2 (L-PBF)  | 22.4          | -     |  |
| Al6061-T6            | 22.6          | 23.0  |  |

# III. Hardware Manufacturing and Development

The LP-DED process can build integral channels within components, providing the ability to significantly reduce part count and eliminate many of the process steps typically required for forming the liner, channel slotting, and closeout of the coolant channels for nozzles. LP-DED is attractive due to these benefits but was at a low technology readiness level (TRL) using thin-wall aluminum alloys prior to RAMFIRE. MSFC's goal was to evaluate the LP-DED technology and mature the process for integral channel wall nozzles, design for LP-DED additive manufacturing, and complete hot-fire testing in relevant environments.

#### A. Nozzle Manufacturing

Two integral channel-cooled nozzles were built using LP-DED printed Al6061-RAM2. The nozzles were produced on an RPM Innovations (RPMI) 557, which provides a build envelop of 5 x 5 x 7 feet (1.52 x 1.52 x 2.13 meters). Each nozzle was designed and printed with a constant rib width, hot-wall, and closeout thickness. A nozzle was printed in 190 hours. The nozzles were built on an ATP-5 aluminum build plate and blue laser scanned prior to removal with a bandsaw. After the removal of the nozzle from the build plate, the nozzle went through HIP and solutioning. The HIP was completed per ASTM-3301-18a [8]. The entire heat treatment cycle and parameters for each step is depicted in Figure 6. Heat treatment is critical to obtain the desired material properties. The process used for LP-DED Al6061-RAM2 is similar to what was developed for L-PBF Al6061-RAM2. The HIP process is a requirement of the NASA-STD-6030 standard to obtain full density and desired fatigue properties [9]. The solution and aging processes were per the industry standard T6 cycle [10]. However, solution was not feasible using water/glycol due to the variations in thickness across regions of the hardware and concerns of distortion, so Argon/Nitrogen quenching was used.

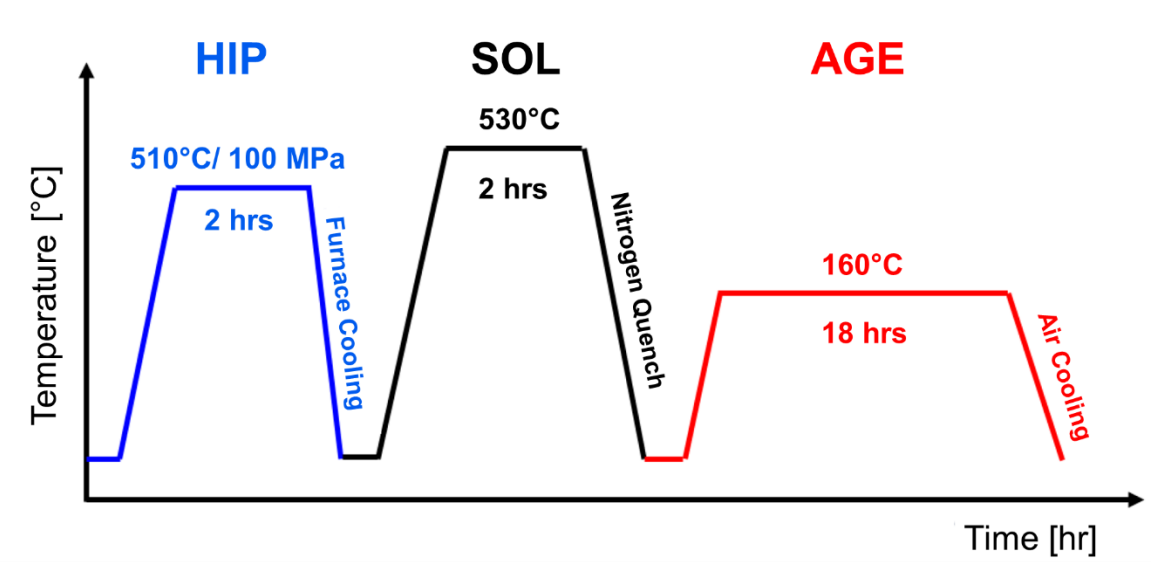


Figure 6. Heat treatment cycle for LP-DED Al6061-RAM2.

Machining of the manifold interfaces was required to prepare the surfaces on the nozzle for electron beam (EB) welding on the forward manifold and Gas Tungsten Arc Welding/Tungsten Inert Gas (GTAW/TIG) welding of the aft manifold. The forward and aft manifolds were traditionally manufactured from Al6061-T6 stock. The forward manifold was machined from extruded bar and the aft manifold was machined from plate. The fuel and temperature/pressure ports were manufactured through an explosive bonding process creating a bimetallic port of Al6061-T6 to Inconel 625 with a tantalum interlayer. The aft manifold and explosively bonded ports were attached using TIG with Al6061-RAM2 filler wire.

The hot-wall was polished using chemical mechanical polishing (CMP) at REM Surface Engineering prior to aging. Up to this point, the manufacturing of the two nozzles was identical. For the aging cycle, Nozzle #1 was aged in a vacuum and Nozzle #2 was aged in open air. Both nozzles were final machined, which included facing the

forward end interface and machining and polishing the seal groove. Nozzle #2 was anodized following final machining. The simplified manufacturing process flow of the nozzles are shown in Figure 7. Select process steps of the nozzles are shown in Figure 8.

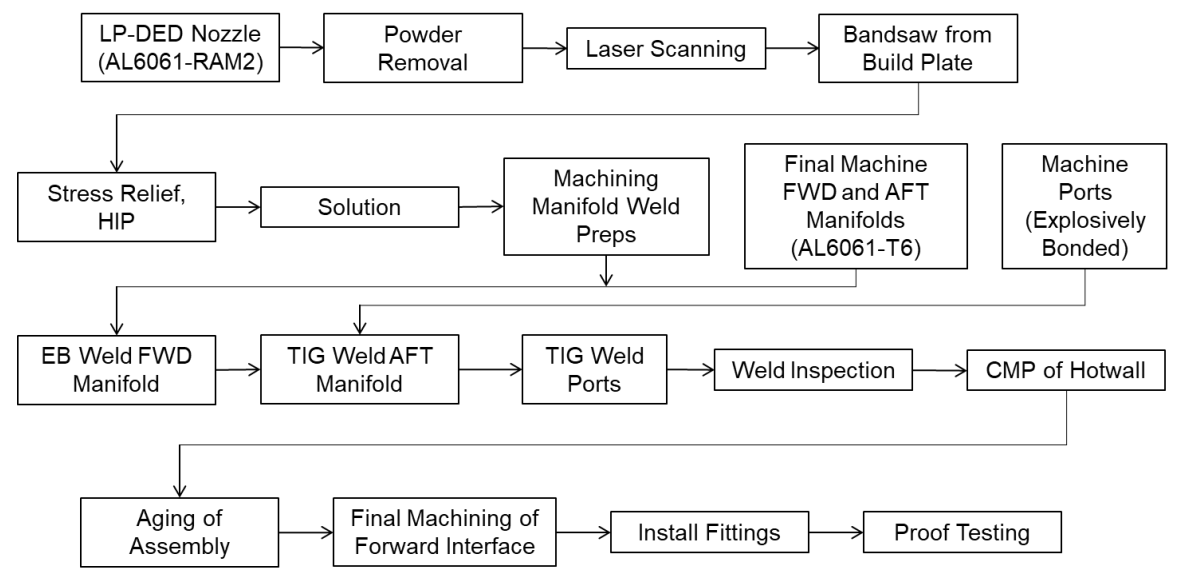


Figure 7. Simplified manufacturing process flow.

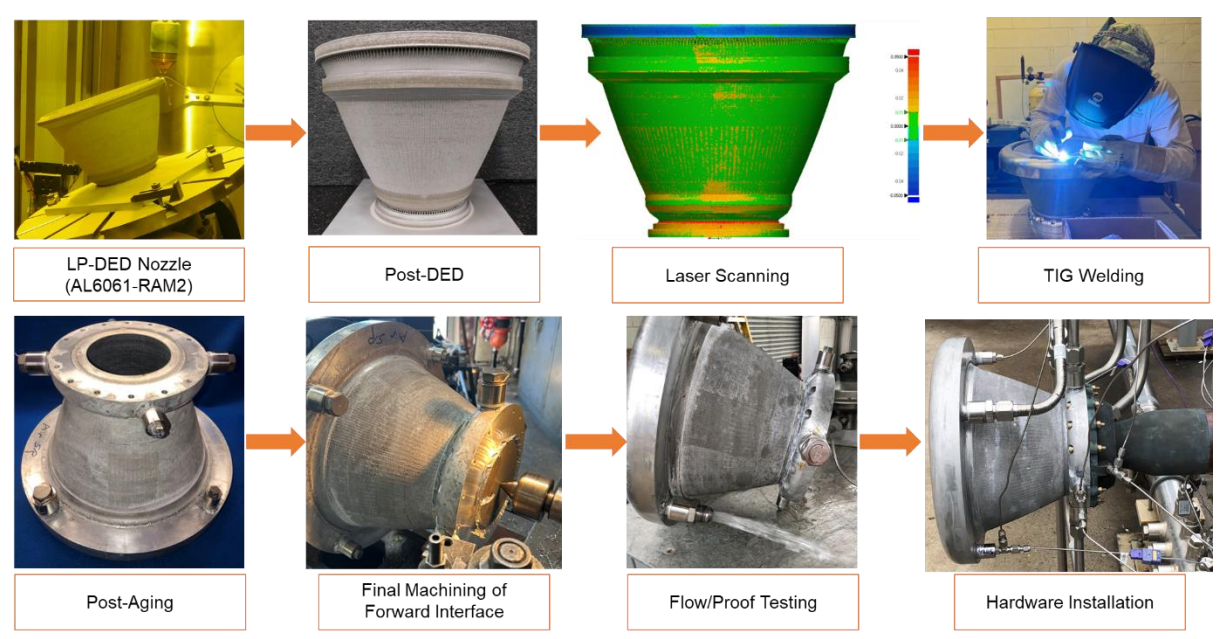


Figure 8. Select nozzle manufacturing steps.

As discussed, Nozzle #2 was anodized after aging of the assembly. Anodization is an electrochemical process that converts the surface of an aluminum material into a natural anodic oxide coating. This oxide coating provides a durable, corrosion-resistant surface and the idea was that this surface would potentially serve as a thermal barrier coating for additional insulation of the hot-wall. Aluminum is typically not used in combustion devices in the hot gas flow path, and there was limited experience with anodization for this environment. The nozzle was delivered to anodization with the explosively bonded Inconel 625 ports already welded onto the manifolds. Anodization is strictly for aluminum, and other materials such as Inconel 625, could be damaged if anodization is attempted. Other (non-

aluminum) materials could also damage the anodization bath/mechanism. Therefore, masking was required on the Inconel 625 ports and the nozzle was successfully anodized per MIL-PRF-8625F Type III Class I anodization and a 0.076 mm (0.003 in.) layer thickness [11]. The anodization processing steps are shown in Figure 9.



Figure 9. Nozzle #2 anodization processing steps.

#### **B.** Welding Development

The nozzles used two different types of welding for attaching the forward and aft manifolds. The forward manifold was mated to the AM nozzle using EB welding. The aft manifold was attached using TIG/GTAW, which requires use of a filler wire.

EB welding of 6000 series aluminum alloys typically requires the addition of filler material (e.g., Al4043) to avoid cracks. However, during EB weld development it was determined that filler material was not required when wrought Al6061-T6 was welded to the base Al6061-RAM2 alloy due to the RAM nano-dispersoids. No gross defects were recorded post-weld, and all welds were visually inspected and satisfactory. The welding development samples indicated the RAM particles in the nozzle were mixed into the fusion zone of the EB weld, reducing cracking susceptibility, which is further supported from observations during TIG welding development.

The RAM technology that allows aluminum alloys to be additively manufactured can be leveraged for welding wire, showing drastic improvements in aluminum weldability. MSFC collaborated with Fortius Metals on the Al6061-RAM2 welding wire and used the technology to weld the aft manifold and ports to the nozzle. The weld team demonstrated high quality welds with the new Al6061-RAM2 filler wire and made a few key observations about the novel Al6061-RAM2 material. These observations included that the new Al6061-RAM2 filler wire exhibited noticeable grain refinement in the weld fusion zone and higher mechanical properties compared to a traditional 4043 filler metal. Additionally, the addition of RAM particles to the solid wire reduced fusion zone cracking when compared to a 6061 wire with no RAM particle additions shown in Figure 10.

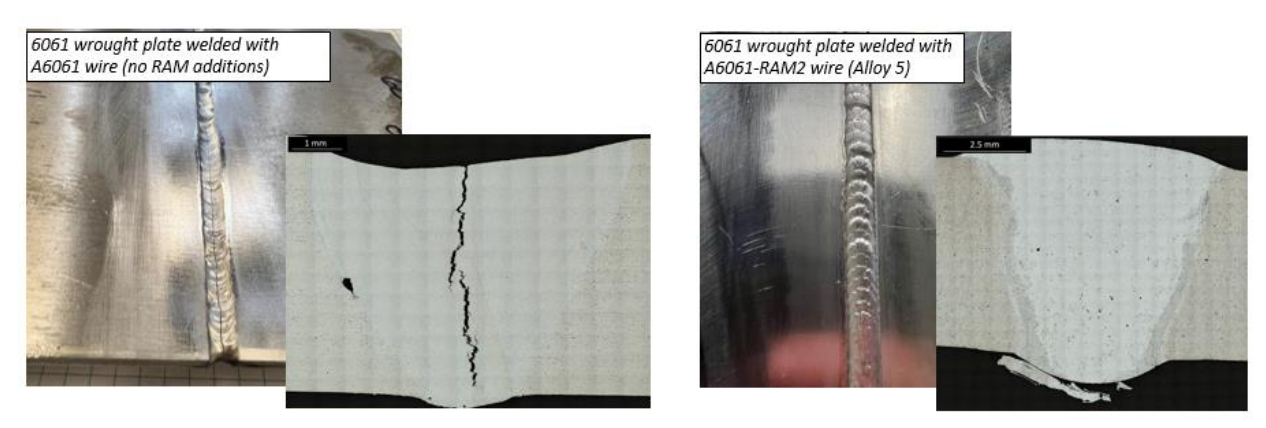


Figure 10. 6061 wrought plates welded with Al6061 wire (No RAM particles) (Left), 6061 wrought plates welded with Al6061-RAM2 wire (Right).

# C. Aluminum/Stainless-Steel Port Development

Pressure cycle and burst testing was conducted to mitigate a risk identified for installing stainless-steel fluid fittings to the aluminum manifolds. The purpose of this testing was to determine the ideal joint to attach the stainless-steel fittings to the Al6061-T6 manifold on the nozzle assembly. The Al6061-RAM2 nozzles were regeneratively cooled using fuel, either LH2 or LCH4. The coolant enters through two ports in the forward manifold and exits from two aft manifold ports, which were designed for common fluid AN-style fittings. Heritage designs typically used stainless-steel or superalloys for the manifolds so threading stainless-steel fittings or welding stainless-steel tubing to the manifolds did not present a risk [2,11]. A vendor survey provided no options for viable aluminium tubing that could be welded to the manifold due to thin walls, small internal diameters, and strength margins required.

Threading stainless-steel directly into an aluminum port could cause galling and leakage at the interface. There was risk of hardware leakage due to coefficient of thermal expansion differences between the two materials at cryogenic temperatures. The low strength of the aluminium threads also limits the load capacity at the joint. Vibrations, inherent to hot-fire testing, cause loosening of threaded connections [13]. The leakage of seals is caused by the loosening of the fastener [14]. During RAMFIRE, the bolts and fittings on the thrust chamber assembly needed to be retorqued several times. The retightening would cause a high amount of wear in the thread contact zone [15]. Typically, to address this issue for bolted joints, a threaded insert of a higher strength material is used. However, that was not an option in the design due to the seal groove of the AS5202 port. A threaded insert could scarf the seal groove during installation. With this evaluation, aluminium threads or tubing were not suitable options.

To mitigate the identified risk, four port test fixtures were fabricated and tested at MSFC. The four test fixtures are shown in Figure 11. Test fixture 1 and 2 are stainless-steel fittings directly threaded into aluminum ports. Test fixture 3 is a stainless-steel fitting threaded into a stainless-steel flange bolted to an Al6061-T6 flange. The Al6061-T6 flange is welded to a Al6061-T6 base with Al6061-RAM2 filler wire. Test fixture 4 is explosively bonded Inconel 625 to Al6061-T6 with a tantalum interlayer. The stainless-steel fitting is threaded into the Inconel 625 and the Al6061-T6 portion of the explosively bonded stock is welded to a Al6061-T6 base with Al6061-RAM2 filler wire.



Figure 11. Test fixtures tested for aluminium to stainless-steel joints.

The fixtures were submerged and pressure cycled with liquid nitrogen, as shown in Figure 12. All fixtures were tested to a minimum of 20 cycles, with each cycle holding the test fixture at 9.0 MPa (1,300 psi) for 5 seconds and 10.8 MPa (1,560 psi) for 15 seconds. After the cryogenic pressure cycling, the fixtures were burst test with ambient temperature water. The number of cycles that the samples were tested to and burst pressure for each test fixture is shown in Table 4. The first two fixtures burst at the interface; the threads of the port galled, and the sealing O-Ring deformed to release the pressure shown in Figure 13. The last two fixtures burst at the aluminium welds shown in Figure 14.



Figure 12. Cryogenic pressure cycle test set-up (Left), test fixture #3 installed in test set-up (Right).

Table 4. Pressure cycle and burst testing results for port development.

| Test Fixture # | Description          | # of   | Burst Pressure |        |  |
|----------------|----------------------|--------|----------------|--------|--|
|                | Description          | Cycles | [MPa]          | [psig] |  |
| 1              | Aluminum Threads     | 30     | 132.3          | 19,193 |  |
| 2              | Aluminum Threads     | 23     | 146.4          | 21,228 |  |
| 3              | <b>Bolted Flange</b> | 24     | 56.1           | 8,142  |  |
| 4              | Explosively Bonded   | 22     | 46.5           | 6,745  |  |



Figure 13. Burst test of test fixture 2.



Figure 14. Burst testing of welded test fixtures. Test fixture 3 (Left), close-up of test fixture 4 (Right).

While test fixtures 1 and 2 did have significantly higher burst pressures than test fixtures 3 and 4, the aluminium threads presented unacceptable risk for continued re-use from engine dynamics. If the threads galled, the hardware would be compromised. It is important to note that the stainless-steel fitting was only torqued once into the fixture; even low-cycle retightening would cause a sharp decline in thread strength (fatigue).

The other two test fixtures burst at the weld seam, which was expected. The burst pressures were both significantly higher than the operating pressure of the nozzle. Of the two, test fixture 4 was selected due to reduced part count and fewer leak paths. The fixture selected used explosion bonding (i.e., explosive welding). Explosion bonding creates a full atomic bond between dissimilar metals and often creates a bond stronger than the principal metals. Explosion bonding uses the controlled detonation of explosives to fuse the two metals together with a flyer plate contacting a base plate. The plasma jet resulting from the wave front of the detonation removes impurities from both metals' surfaces, leaving behind clean metal for joining [16]. Throughout hot-fire testing of the nozzle, the explosively bonded ports remained intact with no leaks or weld cracks.

### D. Demonstration Hardware

A large-scale regeneratively-cooled demonstrator nozzle was built to understand distortion and design complexity at larger scale compared to the nozzle test hardware. The aerospike nozzle was approximately 914 mm (36 in.) in diameter and 762 mm (30 in.) tall. The nozzle was LP-DED printed with Al6061-RAM2 with 1.5 mm (0.060 in.) single-bead wall thickness and took 18 days to print. The demonstration nozzle is shown in Figure 15 with the build direction traversing from the small diameter to the larger diameter. Doghouse features were included at the forward end of the nozzle to help evacuate excess powder in the channels.





Figure 15. Demonstrative large-scale regeneratively cooled nozzle.

A manufacturing demonstration cryogenic tank was also built to showcase complexity with the process and alloy. The tank is approximately 508 mm (20 in.) in diameter and 914 mm (36 in.) tall. The tank was LP-DED printed with Al6061-RAM2 with 1.5 mm (0.060 in.) single-bead wall thickness and took 15 days to print. The demonstration tank is shown in Figure 16. The tank was built using barstock as the build plate to initiate the bottom dome deposition. A series of integral channels were incorporated into the wall to allow for vacuum or cooling for cryogenic tank applications. The barstock was designed to allow for powder to be evacuated from the channels throughout the build duration. The tank body and domes were built as a single piece and dome closeout shown in Figure 16. The trunnion table on the RPMI 557 machine was rotated horizontal to allow for orthogrid ribs to be cladded to the external surface of the tank.



Figure 16. Demonstrative cryogenic tank.

# **IV.** Hot-Fire Testing

The Al6061-RAM2 nozzles were hot-fire tested in relevant environments at the MSFC Test Stand 115 under the PL154 (RAMFIRE) test project. Testing occurred in two subsequent phases – first liquid oxygen/liquid hydrogen (LOX/LH2) propellants and liquid hydrogen as the regenerative coolant; second phase used a liquid oxygen /liquid methane (LOX/LCH4) propellants with liquid methane as the coolant. The tested thrust chamber assembly used two fuel inlets. One inlet was located at the chamber's aft manifold, fuel flowed into the inlet, through the chamber for

cooling, and forward to the injector. Another fuel inlet was located at the nozzle's forward manifold. Fuel flowed into the inlet from the feedline, routed through the nozzle for cooling, and sent to the burn stack after existing the aft manifold. LOX was supplied to one inlet in the injector. An image of the nozzle setup and hot-fire testing is shown in Figure 17.

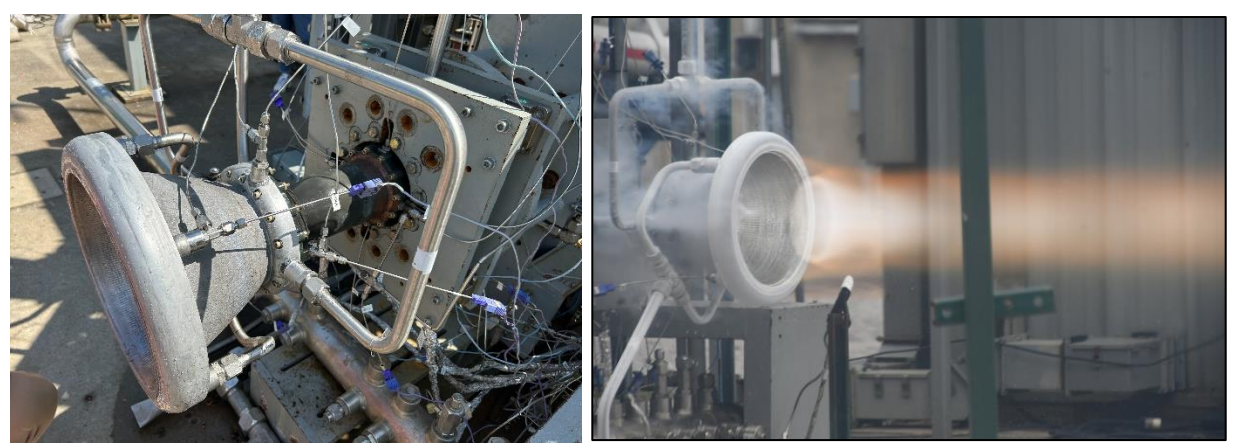


Figure 17. RAMFIRE test assembly. RAMFIRE test assembly with LP-DED Al6061-RAM2 nozzle (left), hot-fire test of Al6061-RAM2 nozzle at MSFC TS115 with LOX/LH2 (right).

The RAMFIRE test project accumulated 577 seconds of mainstage duration and 22 starts on the Al6061-RAM2 nozzles. The non-anodized nozzle was used for hydrogen testing and obtained seven starts with methane. The anodized nozzle subsequently experienced six starts during methane testing. The maximum chamber pressure and mixture ratio during hydrogen testing was 5.7 MPa (829 psia) and MR=7.02. Methane testing had a maximum chamber pressure and mixture ratio of 5.2 MPa (760 psia) and MR=3.65, respectively. Altogether, the non-anodized nozzle amassed 16 starts and 457 seconds of mainstage duration while the anodized nozzle amassed 6 starts and 120 seconds of mainstage. Table 5 provides a summary of the hot-fire statistics for each nozzle as well as the total statistics for the project.

| Nozzle       | Propellant Starts | Ctonto | Mainstage Duration [s] | Max Pc |        | Man MD   |
|--------------|-------------------|--------|------------------------|--------|--------|----------|
|              |                   | Starts |                        | [MPa]  | [psia] | – Max MR |
| Non-Anodized | Hydrogen          | 9      | 302.8                  | 5.7    | 829    | 7.02     |
| Non-Anodized | Methane           | 7      | 154.2                  | 5.2    | 760    | 3.65     |
| Anodized     | Methane           | 6      | 120.0                  | 4.9    | 712    | 3.53     |

577.0

Table 5. Summary of nozzle testing statistics under PL154.

Images of the non-anodized nozzle hardware throughout hot-fire testing are shown in Figure 18. During hydrogen testing, discoloration along a single coolant channel was observed at around 9:30 o'clock. A post-test Computed Tomography (CT) scan confirmed the discoloration was due to trapped powder in the coolant channel. Cooling was adequate and no erosion was observed in this area during methane testing. The ~10x increase thermal conductivity of Al6061-RAM2, compared to superalloys, allowed adequate cooling through adjacent ribs of the blocked channel during test. The region was continuously monitored, discoloration stabilized, and no roughening was detected.

Total

22

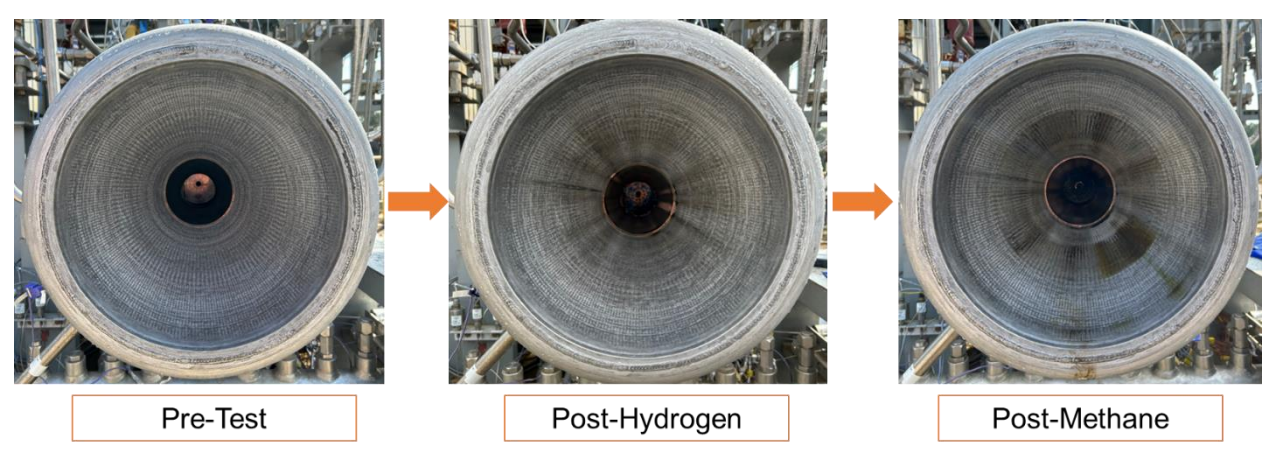


Figure 18. Non-anodized nozzle pre-test, post-hydrogen, and post-methane (7 Starts) testing.

Images of the anodized nozzle throughout methane testing is shown in Figure 19. Some discoloration on the hot-wall was observed. This streaking propagated from the injector and was observed on the chamber as well. There was no roughening or erosion of the hot-wall identified throughout testing. Similar discoloration of the hot-wall was observed on the anodized and non-anodized nozzles with no significant differences between the two.

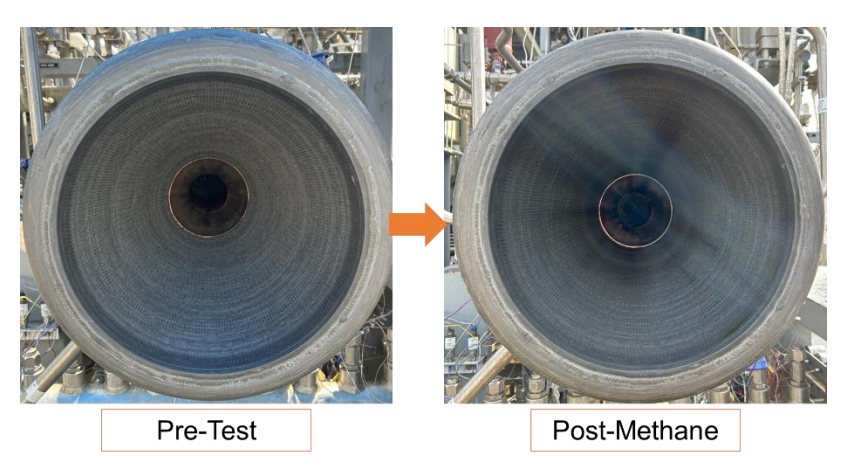


Figure 19. Anodized nozzle pre-test and post-methane testing.

Both nozzles were tested in the same setup throughout the duration of the series. Thorough visual inspections were performed after each test to ensure the nozzles and their associated hardware components (GRCop-42 chambers, GRX-810 injectors, igniters) were acceptable for continued testing. Figure 20 depicts data from a 60 second test using the non-anodized Al6061-RAM2 nozzle with LOX/LH2. Figure 21 presents data from a cycle test that completed two cycles using the anodized Al6061-RAM2 nozzle with methane as the propellant. The two nozzles achieved their testing objectives, proving the performance of the Al6061-RAM2 alloy in high-heat flux environments. Temperatures and pressures were repeatable throughout the campaign providing stable performance throughout mainstage testing. Differential temperatures through the nozzle coolant channels varied by a maximum of 30% for both hydrogen and methane and differential pressures through the nozzle channels varied by a maximum 16% for both propellants.

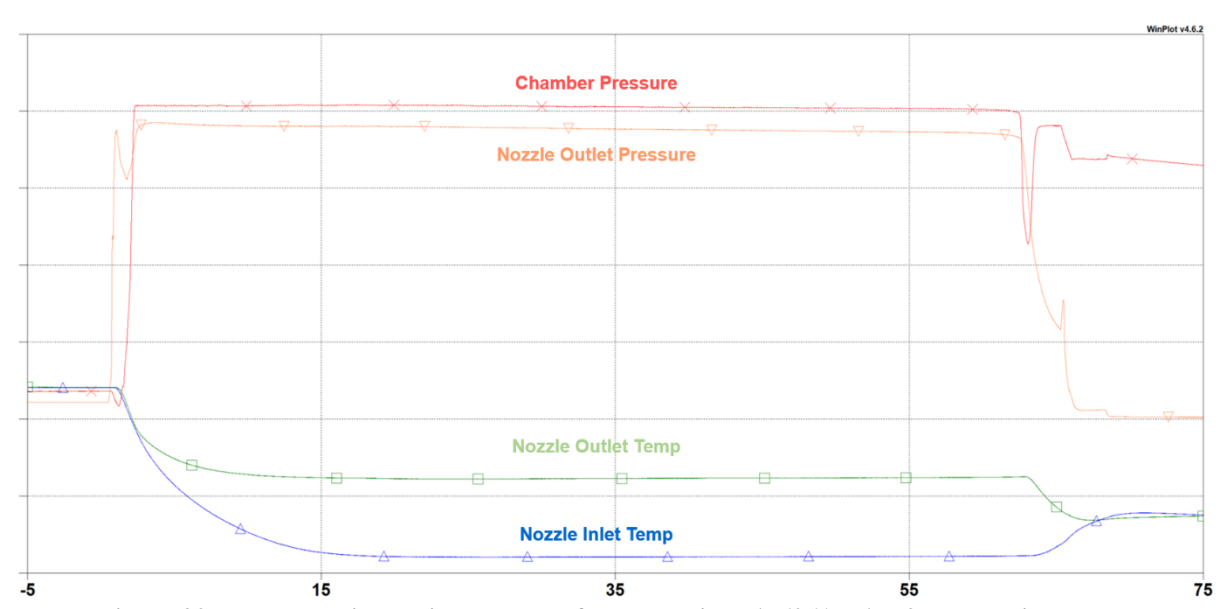


Figure 20. Long duration mainstage test of non-anodized Al6061-RAM2 nozzle with hydrogen.

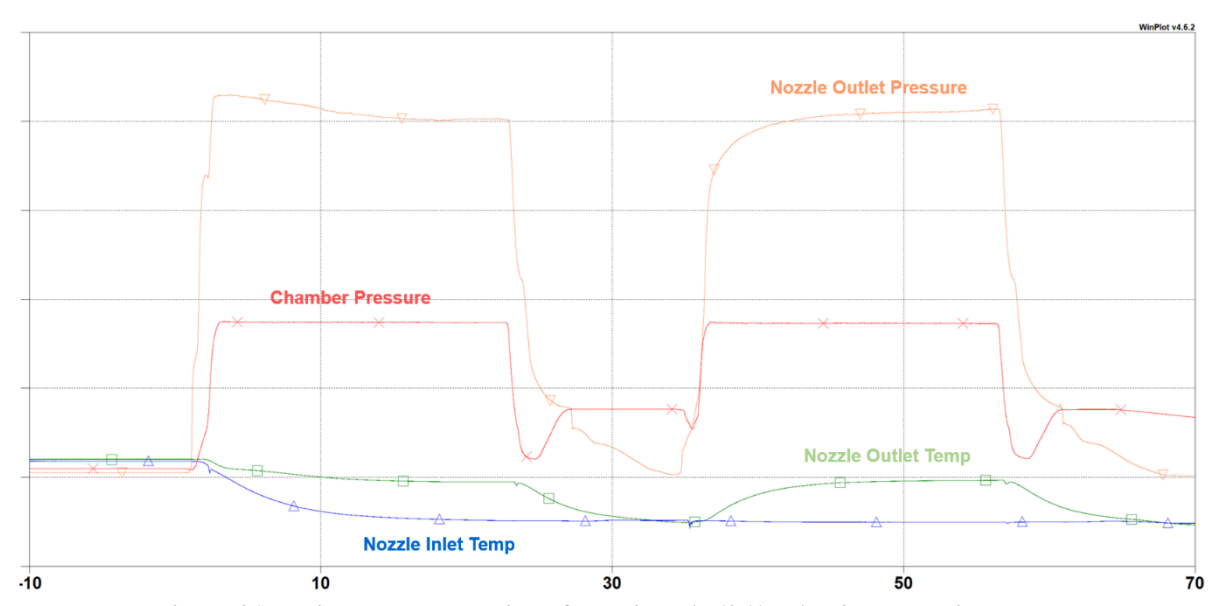


Figure 21. Mainstage cycle testing of anodized Al6061-RAM2 nozzle with methane.

A summary of the data analysis based on the measured parameters of the Al6061-RAM2 nozzles is depicted in Figure 22, Figure 23, and Figure 24. This data includes normalized total heat load compared against the normalized chamber pressure and mixture ratio, as well as normalized differential pressure against nozzle resistance. The data was broken up into three different sets that each corresponded to a different fuel-nozzle combination. Additionally, all data was normalized against a selected value that approximated the mean value of each of the individual data sets.

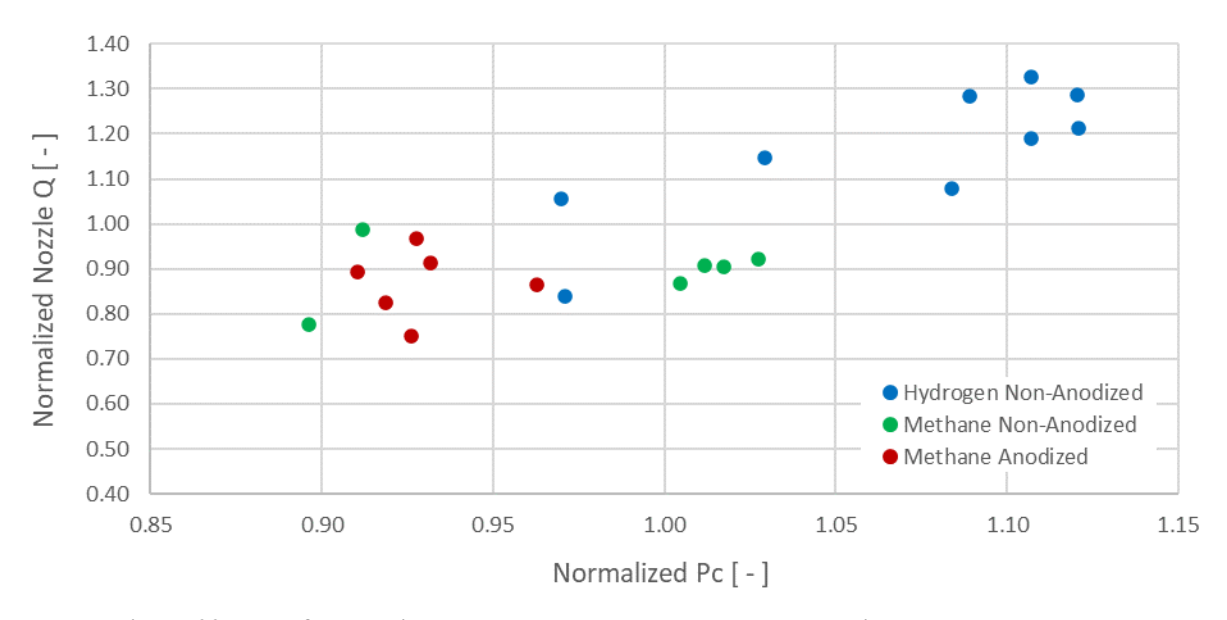


Figure 22. Plot of normalized nozzle total heat load versus normalized chamber pressure.

Normalized total heat load to the nozzle as a function of chamber pressure is represented in Figure 22. The data from both methane and hydrogen appear to follow similar trends. Both display a positive relation as increased chamber pressure leads to increases in the heat load experienced by the nozzle. The relations were as expected because higher chamber pressures increase fluid density, which increases heat load.

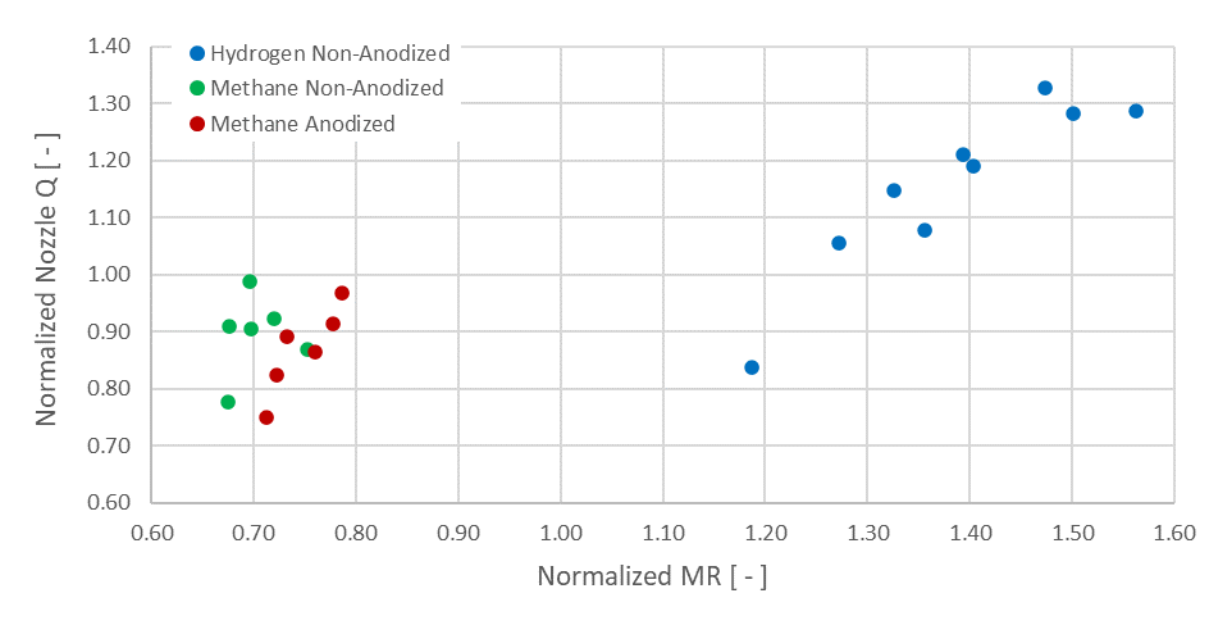


Figure 23. Plot of normalized nozzle total heat load versus normalized mixture ratio.

Normalized total heat load to the nozzle versus normalized mixture ratio is depicted in Figure 23. There is a positive relation between heat load to the nozzle and mixture ratio for both hydrogen and methane, which is expected as propellant combinations approach stoichiometric conditions. The higher reaction temperatures impart a higher heat load to the hardware as anticipated.

Overall, the relationships observed between heat load and chamber pressure as well as mixture ratio behaved as expected. When subjected to representative high heat flux environments, Al6061-RAM2 nozzle performance was predictable and robust within lander class-type rocket engines.

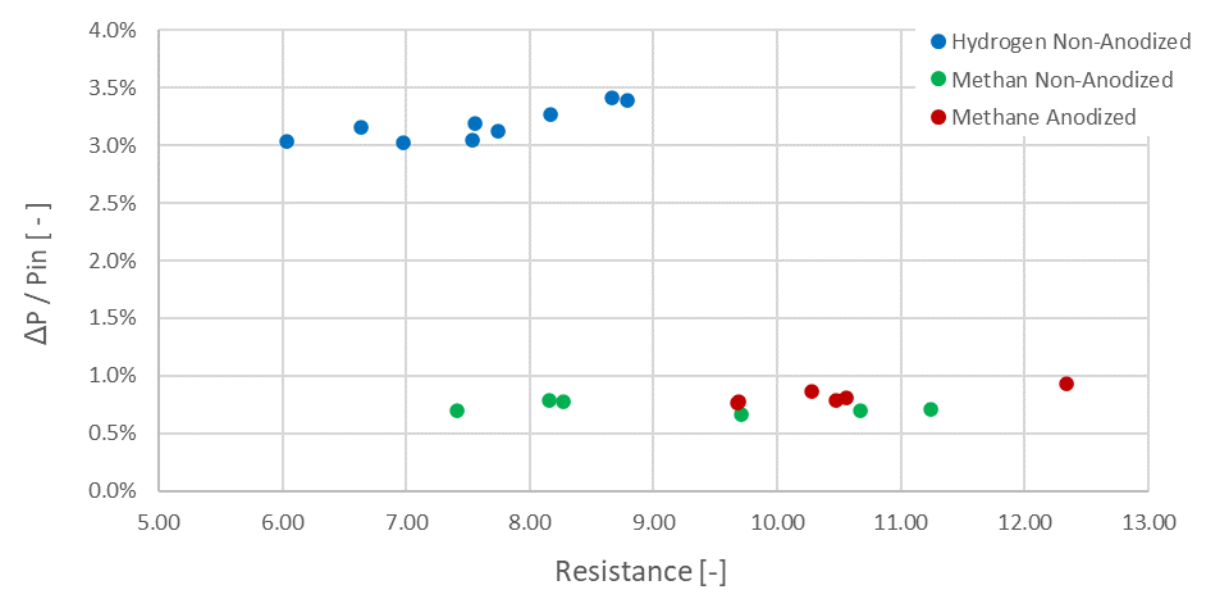


Figure 24. Plot of normalized nozzle pressure drop versus nozzle resistance.

Normalized pressure drop through an individual channel as a function of nozzle resistance is illustrated in Figure 24. In this case, pressure drop has been normalized by the pressure at the inlet of the nozzle manifolds while resistance is an inherently dimensionless number. Resistance is used in this scenario to encapsulate the mass flow rate through an individual channel as well as the density of the fluid in that channel. The pressure drop for both methane and hydrogen were constant at various resistances.

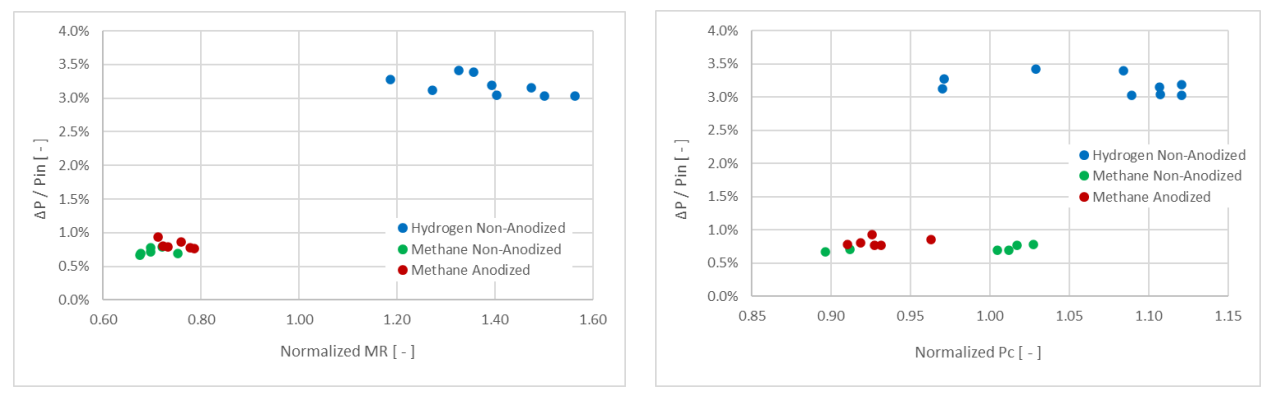


Figure 25. Normalized coolant pressure drop versus normalized mixture ratio (left) and normalized chamber pressure (right).

Further analysis shown in Figure 25 showed that overall pressure drop was also largely independent of both mixture ratio and chamber pressure. This trend and the overall pressure drop values were akin to those seen in a prior test project [1] that used a similar sized LP-DED NASA HR-1 nozzle design.

#### V. Conclusions

NASA and industry partner, Elementum 3D, successfully developed Al6061-RAM2 for the laser powder directed energy deposition (LP-DED) under the Reactive Additive Manufacturing for Fourth Industrial Revolution Exploration Systems (RAMFIRE) project The LP-DED Al6061-RAM2 alloy was matured through additive manufacturing (AM) process development, material characterization and testing, manufacturing technology demonstrators (MTD) and component builds, and successful hot-fire testing. Al6061-RAM2 provides excellent ductility, high strength, and good thermal conductivity targeted for potential use in liquid rocket engine components, cryogenic tanks, and other space structures. The material performed as-expected in a relevant hot-fire test environment for an actively cooled channel wall nozzle sized for 31 kN (7,000 lb<sub>f</sub>) testing. The nozzles tested under the project accumulated 577 seconds of mainstage duration and 22 starts using LOX/LH2 and LOX/LCH4.

The RAMFIRE project completed testing and presented results for chemical composition, powder feedstock parameters, microstructure, mechanical properties, and the coefficient of thermal expansion. Equiaxed, fine grains were observed in all the heat treatment conditions and the mean grain size for LP-DED Al6061-RAM2 is  $\sim$ 5  $\mu$ m, compared to 1.5  $\mu$ m for L-PBF samples. The addition of B4C and Ti inoculant particles provides heterogenous nucleation sites for solidification during the LP-DED process, which causes refinement of the grain structure and formation of equiaxed grains. The vertical and horizontal non-anodized conditions show minor differences in material properties, specifically for ultimate strength, yield strength, and percent elongation. MSFC and industry partners demonstrated that Al6061-RAM2 is a readily printable alloy using large scale additive manufacturing.

Two nozzles were manufactured on the RPMI 557 LP-DED machine and produced in 190 hours each. Several supplemental efforts supported the fabrication of the nozzles including anodization, welding development, and aluminum to stainless-steel joint testing. Welding development corroborated the RAM particles in the nozzle mixed into the fusion zone of the EB weld, reducing cracking susceptibility. Additionally, the Al6061-RAM2 filler wire for TIG welding showed drastic improvements in weldability compared to the traditional 4043 filler wire. The aluminum to stainless-steel joint testing and subsequent hot-fire testing of the nozzle assembly proved the explosively bonded Inconel 625 to Al6061-T6 to be a strong joint and remained intact with no leaks or weld cracks throughout hot-fire testing.

The RAMFIRE test project successfully tested the capabilities of the novel Al6061-RAM2 alloy. The nozzles performed as expected and demonstrated that novel aluminum alloys have the potential for use in high heat flux environments with proper channel design and cooling. The lessons learned and data relative to the LP-DED Al6061-RAM2 alloy are available for industry use.

# VI. Acknowledgements

This paper describes objective technical results and analysis. Any subjective views or opinions that might be expressed in the paper do not necessarily represent the views of the National Aeronautics and Space Administration (NASA) or the United States Government. The results from this study are solely for informational purposes and not an endorsement of any processes by the authors, their employers, or the publishing journal. This work was funded by NASA through an Announcement of Collaborative Opportunity (ACO) under the Space Technology Mission Directorate (STMD) and the Game Changing Development (GCD) program.

Several people are recognized in the advancement, testing, management, and funding to mature the Al6061-RAM2 alloy and subsequent processes. Thank you to our partners involved including Elementum 3D, RPM Innovations (RPMI), Auburn University, REM Surface Engineering, Procam, PTR, Fortius Metals, High Energy Metals, TMC, Advanced Technical Finishing, Pressure Tech, Pinson Valley, and several others. Thank you to the project offices for their support, namely John Fikes. Thank you to several individuals involved in testing: Dennis Strickland, Kendall Feist, Nick Hensley, Steve Baggette, TS115 test crew, and many others involved. Thank you to the individuals who supported aluminum to stainless-steel joint testing: Cody Gilliland, Allen Gatlin, Don Nave, Thomas Ogle, and James Buzzel. Thank you to Will Evans for the work developing the Al6061-RAM2 TIG welding. Thank you to design and analysis support from Kevin Baker, Bob Witbrodt, Brandon Cook and Matt Cross. Thank you to the teams engaged in the materials characterization and testing including MD Faysal Kahn, Colton Katsarelis, Claire Handley, and Gabe Demeneghi. There are also many other individuals involved from NASA and industry – thank you!

#### VII. References

- [1] P.R. Gradl, S.E. Greene, C. Protz, B. Bullard, J. Buzzell, C. Garcia, J. Wood, K. Cooper, J. Hulka, R. Osborne, Additive manufacturing of liquid rocket engine combustion devices: A summary of process developments and hot-fire testing results, 2018 Jt. Propuls. Conf. 2018 (2018) 1–34. https://doi.org/10.2514/6.2018-4625.
- [2] P.R. Gradl, C.S. Protz, T. Wammen, Additive Manufacturing Development and Hot-fire Testing Directed Energy Deposition Inconel 625 and JBK-75 Alloys, 55th AIAA/SAE/ASEE Jt. Propuls. Conf. 2019 (2019) 1–20.
- [3] P.R. Gradl, D. Tinker, B. Williams, T.M. Smith, C. Kantzos, Extreme Temperature Additively Manufactured GRX-810 Alloy Development and Hot-fire Testing for Liquid Rocket Engines, 2023.
- [4] P.R. Gradl, C. Protz, K. Cooper, C. Garcia, D. Ellis, L. Evans, GRCop-42 Development and Hot-fire Testing Using Additive Manufacturing Powder Bed Fusion for Channel- Cooled Combustion Chambers, 55th AIAA/SAE/ASEE Jt. Propuls. Conf. 2019. 2019 (2019) 1–26.
- [5] T. Teasley, P.R. Gradl, M. Garcia, B. Williams, C. Protz, Hot Fire Test Durability of Post Process Polished Additively Manufactured GRCop-alloy Combustion Chambers in LOX/Methane and LOX/Hydrogen, JANNAF. (2021) 1–28.
- [6] Elementum 3D, A6061-RAM2 A6061-RAM2 (Highly Versatile and Cost Effective) Product Information, 1 (2021) 10–12. https://www.elementum3d.com/wp-content/uploads/2021/11/A6061-RAM2-Web-Data-Sheets-2021-04-15.pdf (accessed May 31, 2023).
- [7] J.S. Nuechterlein, J.J. Iten, CA3977288A1, 2016.
- [8] A. International, ASTM F3301-18A Additive Manufacturing Post Processing Methods Standard Specification for Thermal Post-Processing Metal Parts Made Via Powder Bed Fusion, 2018.
- [9] NASA, NASA-STD-6030 Additive Manufacturing Requirements for Spaceflight Systems, 2021. https://ntrs.nasa.gov/citations/20210017082.
- [10] S. International, SAE AMS2772H Heat Treatment of Aluminum Alloy Raw Materials, 2023.
- [11] N.A.S. Command, MIL-PRF-8625F Anodic Coatings for Aluminum and Aluminum Alloy, 2020.
- [12] P.R. Gradl, T. Teasley, C. Protz, C. Katsarelis, P. Chen, Process Development and Hot-fire Testing of Additively Manufactured NASA HR-1 for Liquid Rocket Engine Applications, AIAA Propuls. Energy Forum, 2021. (2021) 1–23. https://doi.org/10.2514/6.2021-3236.
- [13] W. Sun, Z. Guan, Y. Chen, J. Pan, Y. Zeng, Modeling of Preload Bolted Flange Connection Structure for Loosening Analysis and Detection, Shock Vib. 2022 (2022) 25. https://doi.org/https://doi.org/10.1155/2022/7844875.
- [14] W. Zhang, Failure Characteristics and Fault Analysis for Liquid Rocket Engines, 1st ed., Springer Berlin, Heidelberg, 2016. https://doi.org/https://doi.org/10.1007/978-3-662-49254-3.
- [15] T. Hoernig, Increased Thread Load Capability of Bolted Joints in Light Weight Design, SAE Int. J. Mater. Manuf. 11 (2018) 11–22. https://www.jstor.org/stable/26556826.
- [16] P.R. Gradl, Rapid Fabrication Techniques for Liquid Rocket Channel Wall Nozzles, 52nd AIAA/SAE/ASEE Jt. Propuls. Conf. (2016) 1–21.